Plasmonic excitations in metallic nanoparticles: Resonances, dispersion characteristics and near-field patterns

Eugen Tatartschuk,[1] Ekaterina Shamonina,[1,*] and Laszlo Solymar[2]

[1] *Erlangen Graduate School in Advanced Optical Technologies, University of Erlangen-Nuremberg, Paul-Gordan-Str. 6, D-91052, Erlangen, Germany*

[2] *Optical and Semiconductor Devices Group, Electrical and Electronic Engineering (EEE) Department, Imperial College, Exhibition Road, London SW7 2BT, UK*

[*] *Corresponding author: Ekaterina.Shamonina@aot.uni-erlangen.de*

Abstract: Metamaterials acquire their functionality from the structuring of the small building blocks, "artificial atoms". Our paper provides a study of the resonant behaviour for a variety of metallic nanoparticles in the region of hundreds of THz. Resonant modes for nanorods of rectangular cross section are investigated numerically for different types of excitation and the set of resonant frequencies (fundamental and higher order) are determined for rods of various length. From that the dispersion relationship for surface plasmon-polaritons propagating along the rod is deduced. We analyse resonant-mode near-field distribution of the electric field, including the field lines, to emphasise the underlying physics. Resonant frequencies are also found and field distributions analysed when the rods are combined to form particles of L, U and O shapes. The similarities and differences between those particles, both in the values and in the number of resonances, are discussed. The results of this study may aid the design of nanostructured metamaterials with required properties in the IR and optical domain.

OCIS codes: (160.3918) Metamaterials; (240.6680) Surface plasmons; (260.3910) Optics of metals; (290.5850) Scattering, particles; (260.5740) Resonance.

References and links

1. A. Sommerfeld, "Uber die Fortpflanzung elektrodynamischer Wellen langs eines Drahtes," Ann. Phys. Chem. **303**, 233-290 (1899).
2. U. Fano, "The theory of anomalous diffraction gratings and of quasi-stationary waves in metallic surfaces," J. Opt. Soc. Am. **31**, 213-222 (1941).
3. W. O. Schumann, "Ausbreitung elektrischer Wellen langs geschichteter und langs kontinuierlich veranderlicher Plasmen, " Z. Naturforsch. A **5**, 612-617 (1950).
4. A. A. Oliner and T. Tamir, "Backward waves on isotropic plasma slabs," J. Appl. Phys. **33**, 231-233 (1962).
5. E. N. Economou, "Surface plasmas in thin films," Phys. Rev. **182**, 539-554 (1969).
6. D. Sarid, "Long range surface-plasma waves on very thin metal films," Phys. Rev. Lett. **47**, 1927-1930 (1981).
7. J. P. Kottmann, O. J. F. Martin, D. R. Smith, and S. Schultz, "Field polarization and polarization charge distributions in plasmon resonant nanoparticles," New J. Phys. **2**, 271-279 (2000).
8. J. P. Kottmann, O. J. F. Martin, D. R. Smith, and S. Schultz, "Non-regularly shaped plasmon resonant nanoparticle as localised light source for near-field microscopy," J. Microscopy **202**, 60-65 (2001).
9. P. Berini, "Plasmon-polariton modes guided by a metal film of finite width," Opt. Lett. **24**, 1011-1013 (1999).
10. P. Berini, R. Charbonneau, N. Lahoud, and G. Mattiussi, "Characterization of long-range surface-plasmon-polariton waveguides," J. Appl. Phys. **98**, 043109-043120 (2005).
11. S. J. Al-Bader, "Optical transmission on metallic wires-fundamental modes," IEEE J. Quantum Electron. **28**, 325-329 (2004).
12. J. B. Pendry, "Negative refraction makes a perfect lens," Phys. Rev. Lett. **85**, 3966-3969 (2000).
13. E. Shamonina, V. A. Kalinin, K. H. Ringhofer, and L. Solymar, "Imaging, compression and Poynting vector streamlines with negative permittivity materials," Electron. Lett. **37**, 1243-1244 (2001).

#107186 - $15.00 USD Received 4 Feb 2009; revised 26 Mar 2009; accepted 27 Mar 2009; published 5 May 2009

14. S. Linden, C. Enkrich, M.Wegener, J. Zhou, T. Koschny, and C. M. Soukoulis, "Magnetic response of metamaterials at 100 Terahertz," Science **306**, 1351-1353 (2004).
15. S. Zhang, W. Fan, N. C. Panoiu, K. J. Malloy, R. M. Osgood, and S. R. J. Brueck, "Experimental demonstration of near-infrared negative-index metamaterials," Phys. Rev. Lett. **95**, 137404-137407 (2005).
16. V. M. Shalaev, W. Cai, U. K. Chettiar, H.-K. Yuan, A. K. Sarychev, V. P. Drachev, and A. V. Kildishev, "Negative index of refraction in optical metamaterials," Opt. Lett. **30**, 3356-3358 (2005).
17. G. Dolling, M. Wegener, C. M. Soukoulis, and S. Linden, "Negative-index metamaterial at 780 nm wavelength," Opt. Lett. **32**, 53-55 (2007).
18. V. Podolskiy, A. K. Sarychev, and V. M. Shalaev, "Plasmon modes in metal nanowires and left-handed materials," J. Nonlinear Opt. Phys. Mater. **11**, 65-74 (2002).
19. L. V. Panina, A. N. Grigorenko, and D. P. Makhnovskiy, "Optomagnetic composite medium with conducting nanoelements," Phys. Rev. B **66**, 155411-155427 (2002).
20. V. A. Podolskiy, A. K. Sarychev, E. E. Narimanov, and V. M. Shalaev, "Resonant light interaction with plasmonic nanowire systems," J. Opt. A: Pure Appl. Opt. **7**, 32-37 (2005).
21. C. Enkrich, M. Wegener, S. Linden, S. Burger, L. Zschiedrich, F. Schmidt, J. F. Zhou, T. Koschny, and C. M. Soukoulis, "Magnetic metamaterials at telecommunication and visible frequencies," Phys. Rev. Lett. **95**. 203901-203904 (2005).
22. M. Wegener, J. L. Garcia-Pomar, C. M. Soukoulis, N. Meinzer, M. Ruther, and S. Linden, "Toy model for plasmonic metamaterial resonances coupled to two-level system gain," Opt. Express **16**, 19785-19798 (2008).
23. J. S. Shumaker-Parry, H. Rochholz, and M. Kreiter, "Fabrication of crescent-shaped optical antennas," Adv. Mater. **17**, 2131-2134 (2005).
24. J. Aizpurua, P. Hanarp, D. S. Sutherland, M. Käll, G. W. Bryant, amd F. J. García de Abajo, "Optical Properties of Gold Nanorings," Phys. Rev. Lett. **90**, 057401-057404 (2003).
25. K. Busch, G von Freymann, S. Linden, S. F. Mingaleev, L. Tkeshelashvili, and M. Wegener, "Periodic nanostructures for photonics," Phys. Rep. **444**, 101-202 (2007).
26. V. M. Shalaev, "Optical negative-index metamaterials," Nature Photonics **1**, 41-48 (2007).
27. A. Boltasseva and V. M. Shalaev, "Fabrication of optical negative-index metamaterials: Recent advances and outlook," Metamaterials **2**, 1-17 (2008).
28. C. Rockstuhl, T. Zentgraf, H. Guo, N. Liu, C. Etrich, I. Loa, K. Szassen, J. Kuhl, F. Lederer, and H. Giessen, "Resonances of split-ring-resonator metamaterials in the near infrared," Appl. Phys. B **84**, 219-227 (2006).
29. A. Ishikawa, T. Tanaka, and S. Kawata, "Negative magnetic permeability in the visible light region," Phys. Rev. Lett. **95**, 273401-273404 (2005).
30. J. Zhou, T. Koschny, M. Kafesaki, E. N. Economou, J. B. Pendry, and C. M. Soukoulis, "Saturation of the magnetic response of split-ring-resonators at optical frequencies," Phys. Rev. Lett. **95**, 223902-223905 (2005).
31. R. Marques and M. Freire, "On the usefulness of split ring resonators for magnetic metamaterial design at infrared and optical frequencies," IEEE MELECON, Benaldamena (Malaga), Spain, 222-224 (2005).
32. S. Tretyakov, "On geometrical scaling of split-ring and double bar resonators at optical frequencies," Metamaterials **1**, 40-43 (2007).
33. P. B. Johnson and R. W. Christy, "Optical constants of the noble metals," Phys Rev. B **6**, 4370-4379 (1972).
34. H. Jasik, ed., *Antenna Engineering Handbook* (McGraw-Hill, 1961).
35. M. Kafesaki, T. Koschny, R. S. Penciu, T. F. Gundogdu, and E. N. Economou, "Experimental demonstration of negative magnetic permeability in the far infrared frequency region," J. Opt. A: Pure Appl. Opt. **7**, S12-S22 (2005).

1. Introduction

Surface waves have been known for well over a century [1]. Plasma waves on metallic surfaces also go back a long way [2,3]. Major progress came with the work of Oliner and Tamir [4] who were the first to investigate the surface waves on a dielectric-metal-dielectric sandwich. A detailed study of these waves in various configurations was conducted by Economou [5]. For a discussion of the mode with long-range properties see Sarid [6]. Resonances of small triangular elements were studied by Kottmann et al. [7,8]. Metal-dielectric-metal structures of finite cross section, usually referred to as metal stripes or films, have been investigated by Berini [9,10] and Al-Bader [11]. They set up the relevant partial differential equations and solved them numerically subject to the boundary conditions. They chose one particular frequency at which they investigated the dependence of the propagation constant on the geometry, and found a variety of mode structures.

Interest in surface plasma waves has also come from a different direction, from the study of metamaterials. The imaging mechanism of Pendry's 'perfect' lens [12] crucially depends

#107186 - $15.00 USD Received 4 Feb 2009; revised 26 Mar 2009; accepted 27 Mar 2009; published 5 May 2009

on the excitation of surface plasmons [13]. Resonant elements have been an integral part of the research on metamaterials. The frequency of resonance has climbed up in the last few years to 100 THz [14] and more recently to the visible region [15-17]. Novel nanoparticles such as a pair of closely spaced nanostripes or nanorods [18,19], the nanostructured U-particle [20-22], crescent [23] and ring [24] have been introduced. For recent review papers see [25-27]. A detailed study of small resonators in the near infrared was conducted by Rockstuhl et al. [28]. They obtained plasma resonances up to several hundred THz, and they also showed field distributions on nanorods and U-shaped elements. Upper limits of the resonant frequencies based on the concept of kinetic inductance have also been discussed [29-32].

Although resonances in general have received much attention there has been no comprehensive work on the simplest of elements, a single nanorod, and particularly no attempt has been made so far to derive dispersion relations for such a three-dimensional structure. Our first aim is to take a nanorod of square cross section, find its resonant frequencies with the aid of a numerical package (CST Microwave Studio), analyze their field distributions at the fundamental and higher frequencies for a variety of excitations, and find simultaneously the wavelength of the plasma wave in order to derive the dispersion characteristics. The second aim is to extend the search for resonances to structures of other shapes which can be put together by combinations of rods. These are elements of L, U and O shapes, the last one being a rectangular ring.

2. Resonant frequencies and field lines

Our studies will be concerned with rods of square cross section. In the coordinate system of Fig. 1 the length of the rod is equal to l in the y direction, and the sides are at $x = \pm a/2$ and $z = \pm a/2$. For the dielectric constant of the rod as a function of frequency (necessary to specify for time domain simulations) we could give its value in the high frequency region for each value of the frequency from the literature [33]. We have chosen the simpler option of using the lossy Drude model which is not accurate in the vicinity of the plasma frequency but perfectly adequate for our purpose. The chosen variation of the dielectric function is in the form

$$\varepsilon_{\mathrm{p}} = \varepsilon_0 \left[1 - \frac{\omega_{\mathrm{p}}^2}{\omega^2 - \mathrm{i}\gamma\omega} \right], \tag{1}$$

where ε_0 is the free space permittivity, ω and ω_{p} are the frequency and the plasma frequency respectively, and γ is a loss factor, the inverse of the relaxation time. For our simulations we shall take $\omega_{\mathrm{p}} = 1.35 \cdot 10^{16}$ rad/s and $\gamma = 2 \cdot 10^{14}$ rad/s which correspond to those of gold [33].

The excitation is in the form of a plane wave incident in the z direction with its electric field in the y direction, i.e. parallel with the axis of the rod. The numerical package used for finding the resonances is CST Microwave Studio working in the time domain. In the simulations an adaptive meshing was used. The grid step varied from 0.3 nm inside the particles to 8 nm in free space. Open boundary conditions at a distance of 50 nm from the structure were used. The simulation size was around 2 million mesh cells. For the results, obtained in the Section 3, where rods of up to 2000 nm length were simulated, the grid size around the corners was increased to 1 nm and inside the particles to up to 4 nm.

#107186 - $15.00 USD Received 4 Feb 2009; revised 26 Mar 2009; accepted 27 Mar 2009; published 5 May 2009

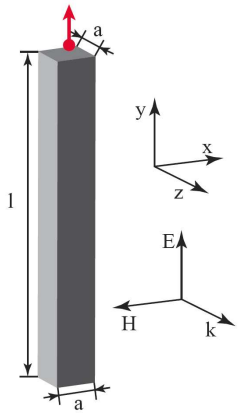

Fig. 1. Schematic representation of the studied nanorod. The *y* component of the electric field measured 4 nm above the top of the rod on the rod axis (red arrow) is used in the plot of the resonance curve.

In all the following studies the cross section of the rod will be taken as equal to $a = 10$ nm. To begin with we shall take a length of $l = 150$ nm. The first three resonances (Fig. 2) are at $f_r = 220$ THz, 541 THz and 749 THz. The electric field lines in the $z = 0$ plane are shown in Figs. 3(a)-(c) for the three frequencies above. The field distributions are symmetric as may be expected from the symmetry of the rod. A possible way of characterising the resonances is to refer to surface charges and to the direction of the electric field at the boundaries. The simplest pattern may be expected at the lowest resonance of 220 THz. As shown in Fig. 3(a) the electric field lines point away from the boundary at the upper part and towards the boundary at the lower part indicating a positive surface charge at the upper and a negative surface charge at the lower part. The surface charge varies along the rod as + −.

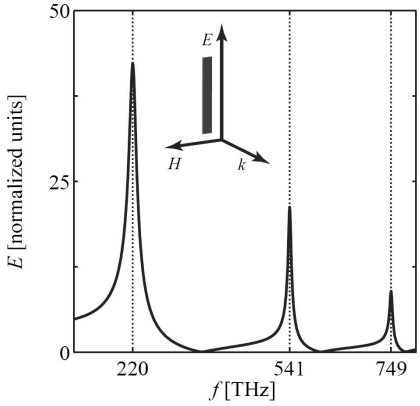

Fig. 2. Resonance curve of the 150 nm long rod normalized to the amplitude of the incident wave. Inset shows the geometry and the polarization of the excitation.

The field lines for the first higher resonance are shown in Fig. 3(b). From the direction of the field lines it may be seen that the surface charges vary along the rod as + − + −. Note that a lower resonance should also exist with surface charges varying as + − + but that cannot be excited by the perpendicularly incident plane wave. The streamlines at the $f_r = 749$ THz resonance are shown in Fig. 3(c). The charge distribution is now + − + − + −. A resonance characterised by a + − + − + distribution is missed again due to the chosen excitation. An alternative description of the resonances is in terms of the zeros of the electric field. There is

#107186 - $15.00 USD Received 4 Feb 2009; revised 26 Mar 2009; accepted 27 Mar 2009; published 5 May 2009

none for the lowest resonance, two for the first higher resonance and four for the next higher resonance.

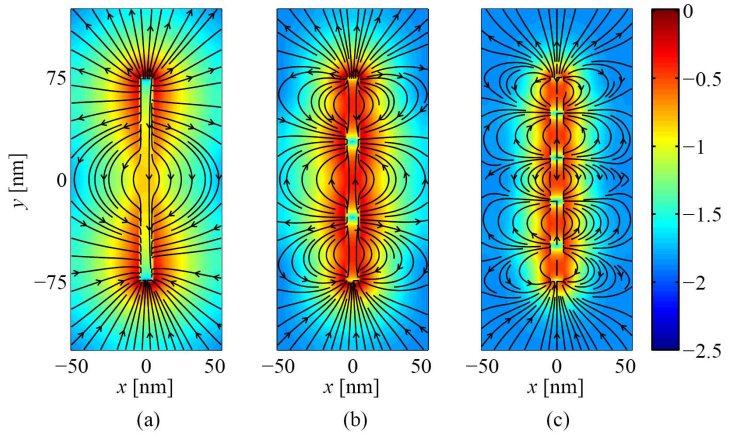

Fig. 3. Electric field patterns of the nanorod at 220 THz (a), 541 THz (b) and 749 THz (c). Field strength plotted on a logarithmic scale (normalized to the respective field maximum).

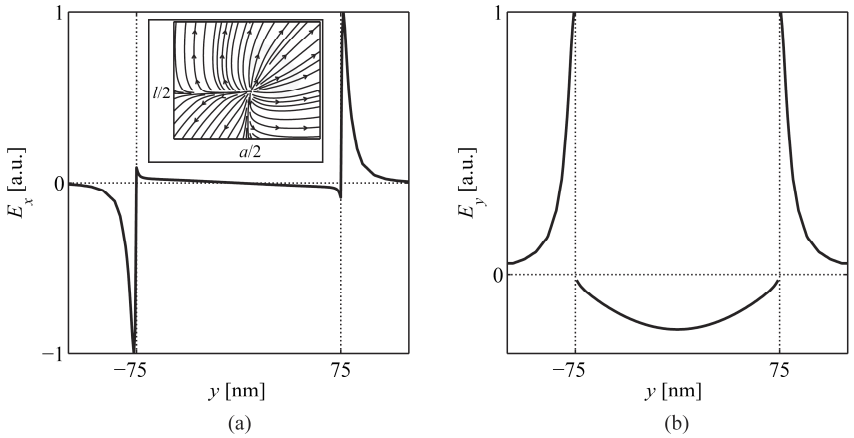

Fig. 4. Electric field components (maxima normalized to unity) along the rod at 220 THz. Inset shows a sketch of the electric field in the vicinity of a corner.

Next we shall plot the variation of E_x and E_y. The E_z component may be disregarded because due to symmetry it should vary in the same manner as E_x. Also, due to symmetry, E_x must be equal to zero along the axis of the rod, at $x = z = 0$. It is therefore plotted (Fig. 4(a)) near to the edge of the rod at $x = 4$ nm, $z = 0$. Since E_x is tangential to the surface at $y = \pm l/2$ it has to be continuous there, and indeed it may be seen to be continuous. The sudden change of sign just beyond the slab indicating a change of direction is far from being obvious. It may though be explained with the aid of the inset where the field lines are shown on a smaller scale. The tangential component of the electric field may be seen to be conserved across the boundary as all field lines move away from the corner both inside and outside of the slab. However the field lines originating in the vicinity of the upper right-hand corner on the surface of the rod must reach the corresponding point in the vicinity of the lower right-hand corner, and they can only do so if they change direction.

Plotting E_y as a function of y (Fig. 4(b)) along the axis (at $x = z = 0$) it may be seen that E_y is discontinuous and changes sign at the two ends of the rod. That occurs because the normal component of the electric displacement must be conserved across the boundary

#107186 - $15.00 USD Received 4 Feb 2009; revised 26 Mar 2009; accepted 27 Mar 2009; published 5 May 2009

$$\varepsilon_{\text{air}} E_{y,\text{air}} = \varepsilon_{\text{p}} E_{y,\text{p}}, \tag{2}$$

where $E_{y,\text{air}}$ and $E_{y,\text{p}}$ are the y components of the electric field just outside and just inside the rod. Note that in eqn (2) we relied on the equivalent dielectric constant as given by the Drude model. The corresponding physical explanation is that the electric field changes sign because the dielectric constant in the metal is negative. A more direct, and less formal, physical explanation would invoke the existence of surface charges on the metal air boundary, saying that the electric field lines must end up on the surface charges, and the difference of the electric flux densities on the two sides must be equal to the surface charge. The variation along the x axis of E_x for $y = 74$ nm, $z = 0$ and of E_y for $y = z = 0$ is plotted in Figs. 5(a) and (b). It is now the E_x component that is discontinuous and E_y that is continuous at the boundary, $x = \pm a/2$. The variation of the same components as a function of y for the two higher orders is shown in Figs. 6 and 7.

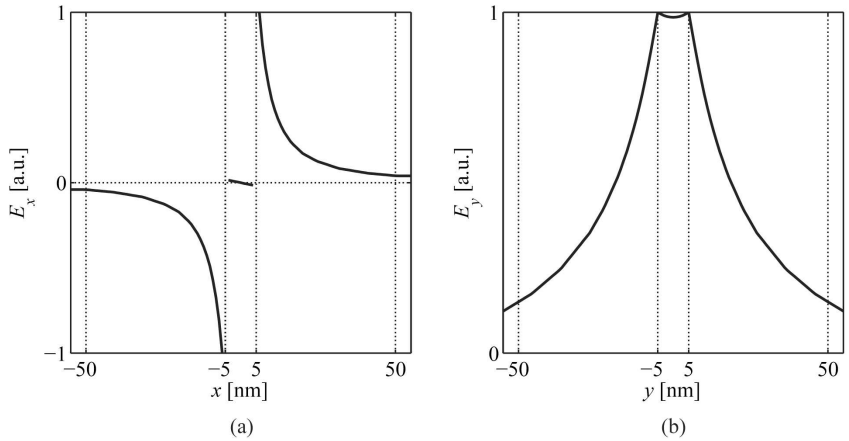

Fig. 5. Electric field components (maxima normalized to unity) across the rod at 220 THz.

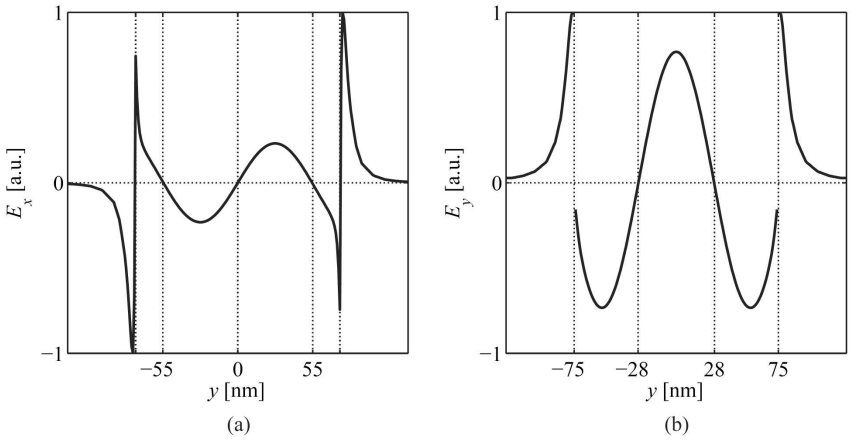

Fig. 6. Electric field components (maxima normalized to unity) along the rod at 541 THz.

#107186 - $15.00 USD Received 4 Feb 2009; revised 26 Mar 2009; accepted 27 Mar 2009; published 5 May 2009

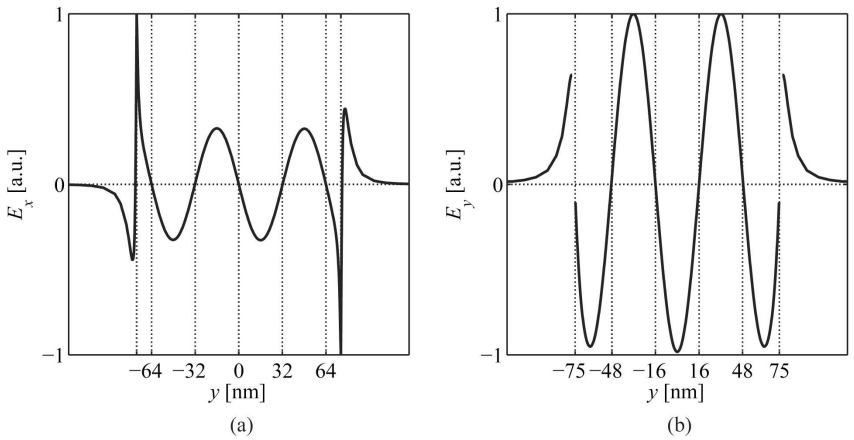

Fig. 7. Electric field components (maxima normalized to unity) along the rod at 749 THz.

3. Dispersion relations

In Fig. 6(a) the range between $y = -55$ nm and $y = 55$ nm shows one period of a sine function which gives us immediately the wavelength of the plasma wave to be equal to 110 nm. This is exactly what we have been looking for. Our aim has been to find the dispersion curve, the $\omega - k$ relationship in a plasma rod of 10 nm × 10 nm cross section. We know now that at a frequency of 541 THz the value of k is equal to $2\pi/110\text{ nm} = 5.7\cdot10^7\text{ m}^{-1}$. The same kind of information could be deduced also from Fig. 7(a) where two periods are shown. In this case the plasma wavelength is 64 nm at a frequency of 749 THz giving another point on the dispersion curve.

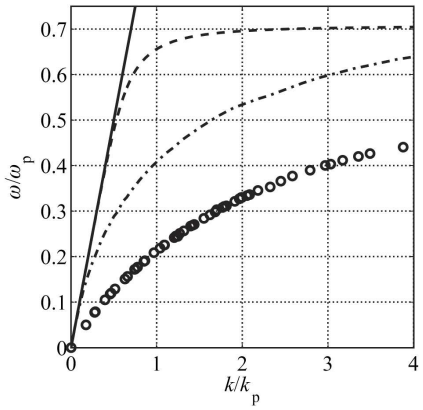

Fig. 8. Comparison of the dispersion curves of a metal-air interface (dashed curve), a 10 nm thick metal slab (dashed-dotted curve) and the retrieved dispersion of the 10 nm × 10 nm thick rod (open circles). Solid curve is the light line.

For finding the resonances at lower frequencies we need to choose longer rods but otherwise it is straightforward to find the dispersion curve. The general rule is that by relying on the fundamental and higher resonant frequencies we can obtain the plasma wavelengths which correspond to the resonant frequencies. The dispersion curve found by this method is shown in Fig. 8 (open circles) against k/k_p, the normalised wave number, where $k_p = \omega_p/c = 4.6\cdot10^7\text{ m}^{-1}$. For comparison we plot there also the dispersion curve of a single plasma-air boundary (dashed lines) and the lower branch of the dispersion curve of a 2D slab of plasma with boundaries 10 nm apart. (Due to splitting there must be a branch not only

#107186 - $15.00 USD Received 4 Feb 2009; revised 26 Mar 2009; accepted 27 Mar 2009; published 5 May 2009

below but also above the single-boundary curve but that is of no interest in the present context.) A slab has two free surfaces, a rectangular rod has four. Hence the lowest branch of the dispersion curve of the rod will lie further away from the unperturbed dispersion of the single metal-air interface, i.e. below the lower branch of the dispersion curve of the slab (see Fig. 8).

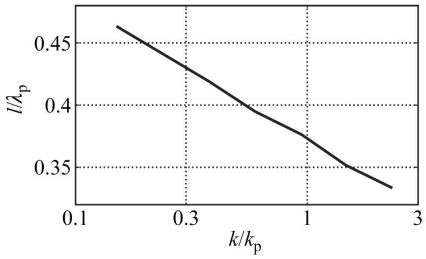

Fig. 9. Resonant length of the rod at its lowest resonance.

What can we say about the length of the rod in terms of wavelength at the lowest resonance? At its resonant frequency, f_r = 220 THz, the corresponding plasma wavelength can now be obtained from Fig. 8. It is λ_p = 370 nm coming to $l = 0.4\lambda_p$. We can repeat the exercise by taking rods of different lengths. The resonant length may be expected to depend on the plasma wavelength, and indeed this is the case. As k/k_p increases the length of the rod in terms of the plasma wavelength declines as shown in Fig. 9. The explanation we may offer is that when the wave resembles a plane electromagnetic wave then the rod's first resonant length should be a little below half-wavelength as it follows from low-frequency antenna theory (see e.g. [34]). The decline of the resonant length with increasing k/k_p is probably due to the fact that with decreasing plasma wavelength the two end surfaces will also influence the total length at resonance.

4. Combination of rods

Next we look at the resonant frequencies of a combination of rods (see Fig. 10) which we shall call the L, U and O configurations. The cross section is still equal to 10 nm × 10 nm, and in each case l = 80 nm.

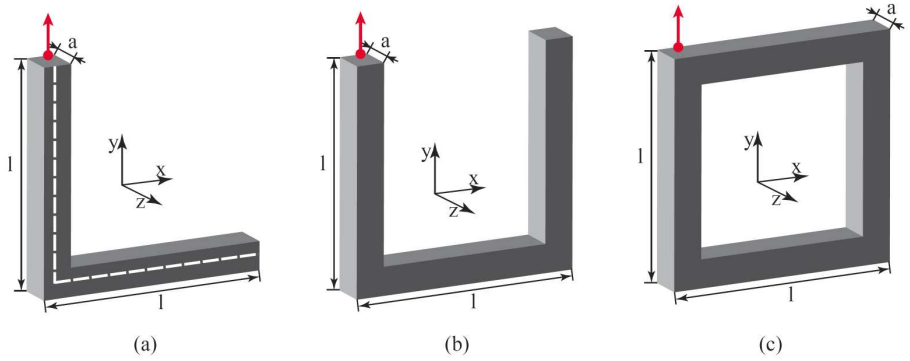

Fig. 10. Schematic representation of the L, U and O particles. The y component of the electric field measured 4 nm above the left vertical rod on its axis (red arrow) is used in the plot of the resonance curves.

#107186 - $15.00 USD Received 4 Feb 2009; revised 26 Mar 2009; accepted 27 Mar 2009; published 5 May 2009

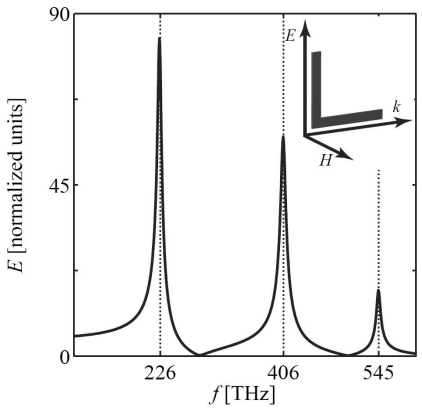

Fig. 11. Resonance curve of the 150 nm long L particle normalized to the amplitude of the incident wave. Inset shows the geometry and the polarization of the excitation.

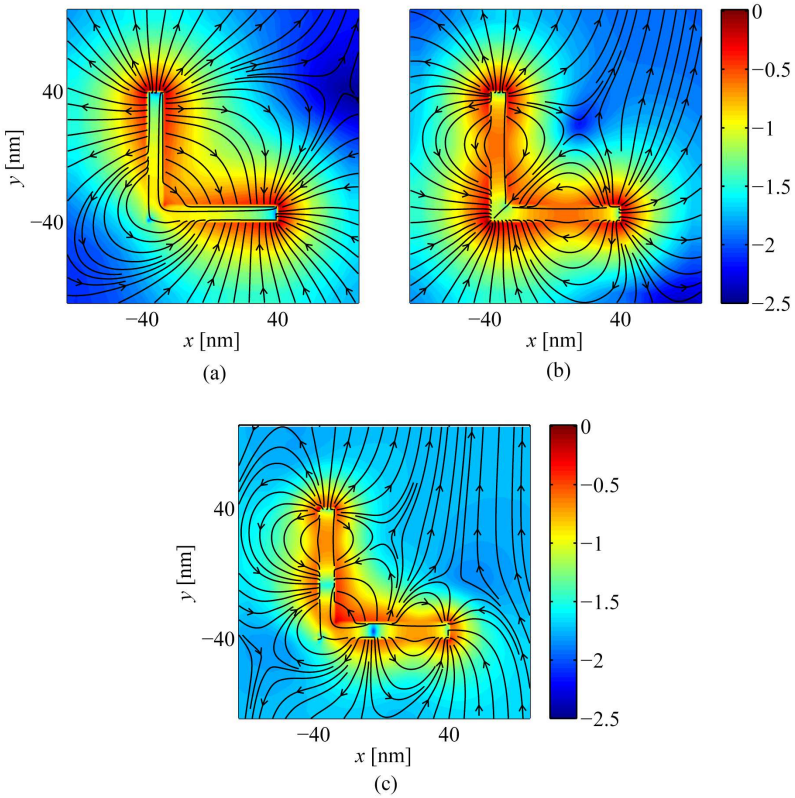

Fig. 12. Electric field patterns of the L particle at 226 THz (a), 406 THz (b) and 545 THz (c). Field strength plotted on a logarithmic scale (normalized to the respective field maximum).

L configuration. The total length of the L particle (measured along the dashed line of Fig. 10(a)) is equal to 150 nm, the same length as that of the rod studied earlier. The first three resonances at 226 THz, 406 THz and 545 THz are shown in Fig. 11. The lowest resonance at 226 THz is very close to that of the rod of the same length. It may therefore be reasonably expected that the field distribution will also be in some way similar. This is indeed so as may be seen in Fig. 12(a). As the rod is bent into the L shape the field distribution more or less

#107186 - $15.00 USD Received 4 Feb 2009; revised 26 Mar 2009; accepted 27 Mar 2009; published 5 May 2009

follows it. The next resonance at 406 THz is the one missing for the rod. The field lines are shown in Fig. 12(b). Since the L particle is asymmetrically excited the + − + resonance may now be present. The resonance at $f_r = 545$ THz (field lines plotted in Fig. 12(c)) is again the bent equivalent of that shown in Fig. 3(c).

U configuration. The total length along the centres of the rods amounts to 220 nm. Whether a particular resonance is present or absent will depend on the excitation. Let us start with the excitation shown in the inset of Fig. 13, the electric field being parallel with the horizontal part of the U and the magnetic field perpendicular to the plane of the U. The resonant frequencies are 162 THz and 418 THz. The field lines corresponding to the lowest resonance are shown in Fig. 14(a). It may be seen that the field lines between the vertical sides of the U are practically horizontal, the same kind as in a capacitor. The currents flowing through the metal part are certainly related to the inductance so this resonance may be called an *LC* resonance as done for example by Rockstuhl et al. [28]. On the other hand we may argue that this is the same type of plasma resonance as those found before. The charge distribution from one end to the other end is + − and the electric field does not vanish in between. To check this we worked out the lowest resonant frequency of a rod of 220 nm (obtained by straightening out the U) and found it equal to 162 THz, the same value. Thus if the resonance for the rod is a plasma resonance then the resonance for the U should also be regarded as a plasma resonance. However the argument could be inverted. If the resonance for the U is an *LC* resonance then the analogous resonance for the rod should also be an *LC* resonance. After all even for a rod (see Fig. 3(a)) field lines move from positive charge to negative charge as in a capacitor so why should we not regard it a capacitor? It is quite possible that using a generalized definition of capacitance many of the resonances found could be described in terms of some equivalent inductor and capacitor, but it is far from obvious how to do that. We ourselves believe that the dominant physical mechanism is the propagation of surface plasmon-polaritons (for a brief discussion see the end of this Section).

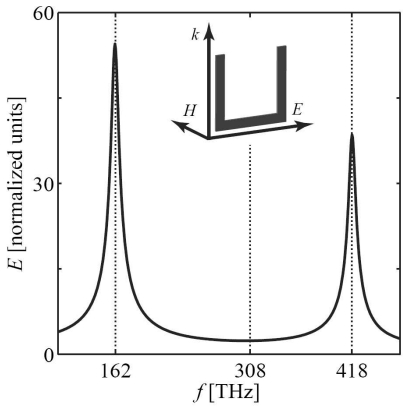

Fig. 13. Resonance curve of the 220 nm long U particle normalized to the amplitude of the incident wave. Inset shows the geometry and the polarization of the excitation.

The field lines for the resonance at 418 THz are shown in Fig. 14(c). The pattern is analogous with that in Fig. 3(b). The field lines appear to follow the twice-bent shape of the U. Correspondent resonance with this charge distribution along the 220 nm long rod can be found at 416 THz, a close value.

Next we shall look at excitation by a plane wave incident in a direction perpendicular to the plane of the U (see inset of Fig. 15) with the electric field parallel with the horizontal side of the U. The resonance curves shown in Fig. 15 are practically identical with those in Fig. 13. The conclusion is that what matters is the electric field. It makes no difference whether the magnetic field is perpendicular to or is in the plane of the U.

#107186 - $15.00 USD Received 4 Feb 2009; revised 26 Mar 2009; accepted 27 Mar 2009; published 5 May 2009

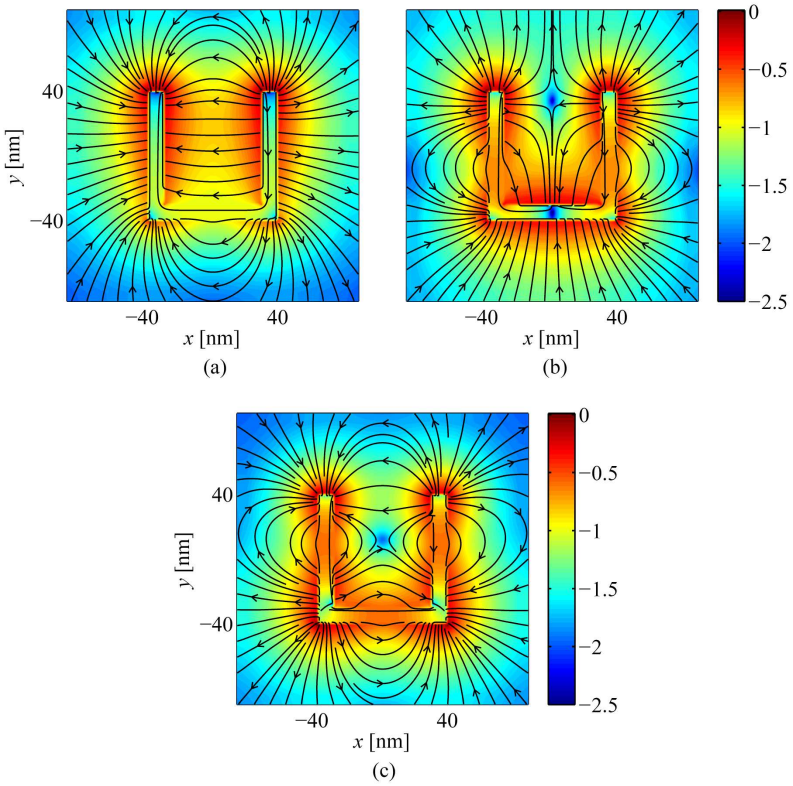

Fig. 14. Electric field patterns of the U particle at 162 THz (a), 308 THz (b) and 418 THz (c). Field strength plotted on a logarithmic scale (normalized to the respective field maximum).

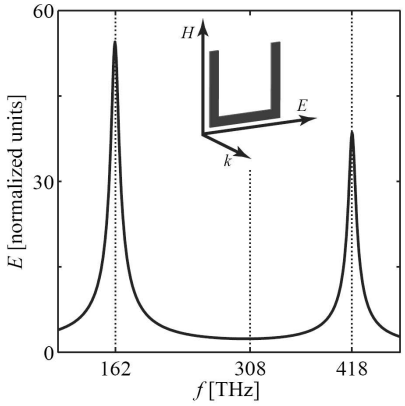

Fig. 15. Resonance curve of the U particle normalized to the amplitude of the incident wave. Inset shows the geometry and the polarization of the excitation.

The resonance curve for perpendicular incidence when the electric field is parallel with the side of the U is shown in Fig. 16. There is now only one resonance at 308 THz. This is again a field pattern which cannot be excited on a rod but it is possible for the U. The charge distribution (see Fig. 14(b)) is + − +, and the electric field has a zero at the centre of the horizontal part of the U. Qualitatively, it is the same type of resonance as that in Fig. 12(b) for the L. Again we can say that the resonance only depends on the overall length of the particle.

#107186 - $15.00 USD Received 4 Feb 2009; revised 26 Mar 2009; accepted 27 Mar 2009; published 5 May 2009

It does not correspond to the resonance of the 80 nm long rod. Note that the resonances at 162 THz and at 418 THz are not excited.

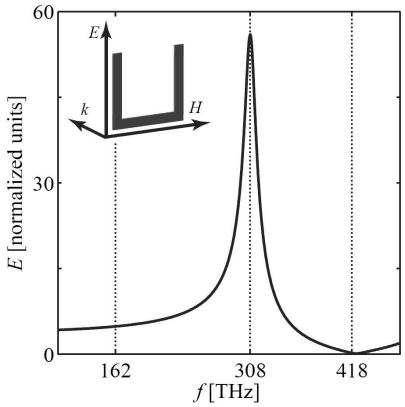

Fig. 16. Resonance curve of the U particle normalized to the amplitude of the incident wave. Inset shows the geometry and the polarization of the excitation.

Finally we shall look at the excitation as shown in the inset of Fig. 17. The electric field is still parallel with the vertical side but the magnetic field is perpendicular to the plane of the U. All three resonances may now be seen although the lowest and the highest resonance are only weakly excited.

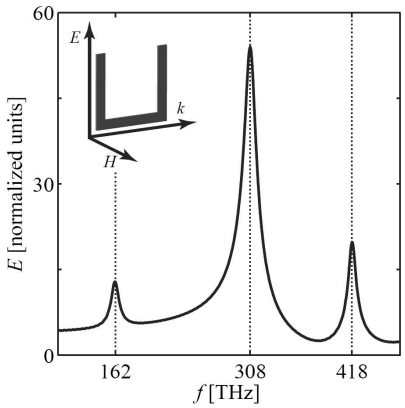

Fig. 17. Resonance curve of the U particle normalized to the amplitude of the incident wave. Inset shows the geometry and the polarization of the excitation.

O configuration. The structure under investigation is now a ring made up by the same rods. With this geometry one may expect resonances when the total length is equal to an integral number of plasma wavelengths. The first three resonances obtained are plotted in Fig. 18 for the two possible polarisations. At the three resonances of 279 THz, 463 THz and 601 THz the corresponding plasma wavelengths may be obtained from the dispersion curve of Fig. 8. They are with good approximation $\lambda_p = 280$ nm, 140 nm and 93 nm corresponding clearly to one, two and three plasma wavelengths at the average perimeter length of 280 nm. The field lines are shown in Figs. 19(a)-(c). The charge distributions are $+-$ at 279 THz, $+-+-$ at 463 THz and $+-+-+-$ at 601 THz. The highest and lowest resonances are independent of the polarisation of the exciting plane wave.

#107186 - $15.00 USD Received 4 Feb 2009; revised 26 Mar 2009; accepted 27 Mar 2009; published 5 May 2009

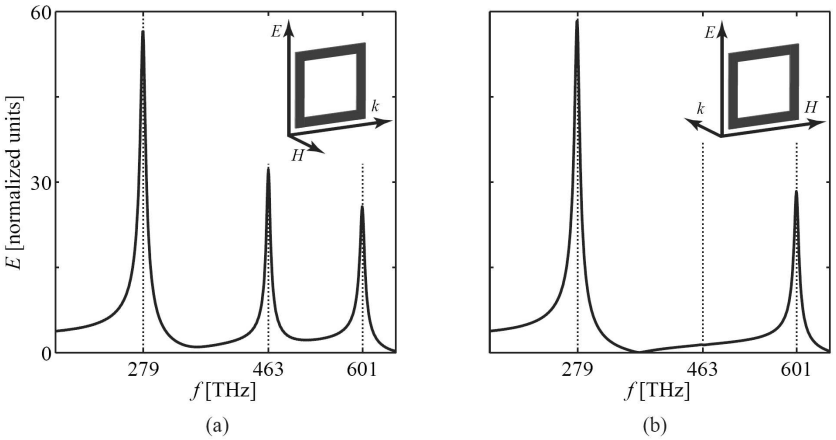

Fig. 18. Resonance curves of the 280 nm long O particle normalized to the amplitude of the incident wave, for two different polarizations of the excitation.

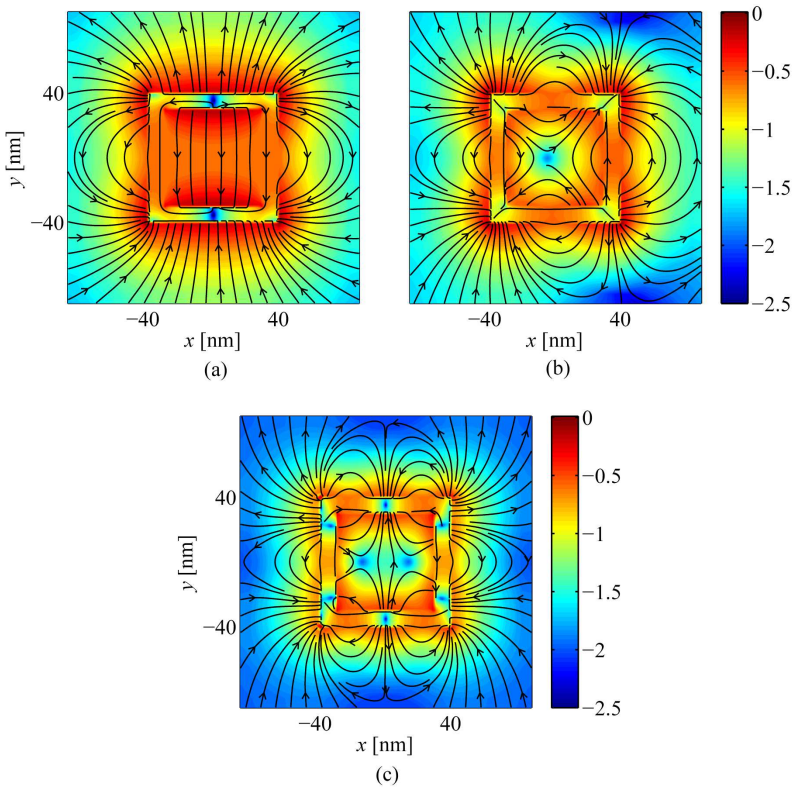

Fig. 19. Electric field patterns of the O particle at 279 THz (a), 463 THz (b) and 601 THz (c). Field strength plotted on a logarithmic scale (normalized to the respective field maximum).

One might ask whether the physical reason for the resonance at 463 THz is the current induced by the magnetic field perpendicular to the plane of the particle. Or is it the lack of symmetry of the electric field component in the left and the right halves of the U due to the plane wave incident from the left? To clarify this we have performed another simulation (not

#107186 - $15.00 USD Received 4 Feb 2009; revised 26 Mar 2009; accepted 27 Mar 2009; published 5 May 2009

shown here) with the magnetic field in the particle plane, $\vec{H} \| [110]$, and the propagation direction $\vec{k} \| [1,-1,\sqrt{2}]$ having an in-plane component (for coordinate system see Fig. 10(c)). In this configuration magnetic excitation is not possible [35], and yet the same set of three resonances as in Fig. 18(a) was observed proving the non-magnetic nature of the second resonance at 463 THz.

We have also made simulations with regular polygons but that did not lead to any new information. Resonances depended on the total average perimeter in the same way as for the O particle.

A note on the nature of the resonances found. When the analysis of a set of physical phenomena is done with the aid of simulations there is no absolute certainty as to the physical mechanism. When we talk about a physical mechanism what we usually mean is that such-and-such a set of equations yields some results which we regard authentic once confirmed by experiments. We explain then the physics by translating into ordinary language what the mathematics tells us. If the model consisted of a combination of metal/air interfaces and the equations involved charge densities and currents in addition to propagating electric and magnetic fields along the interfaces, then the accepted custom is to call those waves Surface-Plasmon-Polaritons. The evidence that in the present paper the dominant mechanism is due to SPPs is that by gradually increasing the rod dimension in the x direction, while keeping the same rod thickness in the z direction, the dispersion curve tends towards that of SPPs on a 10 nm thick metal slab. Further evidence is provided by the similarity of our results to those of Berini [9] and Al-Bader [11] who relied on the solution of the relevant partial differential equations.

5. Conclusions

The properties of waves on a plasma rod of $10\,\text{nm} \times 10\,\text{nm}$ cross section have been investigated with the aid of the numerical package CST Microwave Studio. Field distributions at resonant frequencies have been analyzed and the dispersion curve up to a wave number of $k = 4\omega_p/c$ has been extracted. It has been shown that, the surfaces being strongly coupled, the dispersion curve for the rod is below that of a slab of 10 nm thickness. The length of the rod at the lowest resonance has been found to be below half-wavelength and is shown to decline as the wave number increases. The study of field patterns has been extended to combinations of rods in the shape of L, U and O particles. Resonance curves for input plane waves of various directions and polarisations have been studied. The relations between the total length of the particle and the available resonances have been examined. The nature of the resonances, whether a plasma or an *LC* resonance, has been discussed.

Acknowledgments

E. T. and E. S. gratefully acknowledge funding by the German Research Foundation (DFG) within the Erlangen Graduate School in Advanced Optical Technologies (SAOT) and the Emmy Noether-Programme.

#107186 - $15.00 USD Received 4 Feb 2009; revised 26 Mar 2009; accepted 27 Mar 2009; published 5 May 2009